Pergamon

Tetrahedron 56 (2000) 6707–6719

TETRAHEDRON

Hexagonal Nanoporous Host Structures Based on 2,4,6-Tris-4-(halo-phenoxy)-1,3,5-triazines (Halo=Chloro, Bromo)

Ram K. R. Jetti,[a] Praveen K. Thallapally,[a] Feng Xue,[b] Thomas C. W. Mak[b,*] and Ashwini Nangia[a,*]

[a]*School of Chemistry, University of Hyderabad, Hyderabad 500 046, India*

[b]*Department of Chemistry, The Chinese University of Hong Kong, Shatin, New Territories, Hong Kong SAR, People's Republic of China*

Received 11 January 2000; accepted 13 April 2000

Abstract—Based on our earlier observation that *para*-halogenated phenoxy triazines self-assemble as hexagonal nanoporous frameworks, this study deals with the inclusion of structurally related guest species in the one-dimensional channels of the title host compounds. A systematic analysis of six isomorphous, X-ray crystal structures (space group $P6_3/m$) provides valuable information of wide-ranging implications in host–guest chemistry: (1) construction of a host lattice with weak intermolecular interactions; (2) correlation of guest-size and host–channel area with order/disorder in the host; (3) role of molecular symmetry and multi-point hydrogen bond recognition for ordered guest species; (4) unusual structural behaviour and properties of guests constrained in a narrow channel. Lastly, a ternary adduct crystal shows an intricate hydrogen bonding network in the polar space group R3c with a super-cell of c=63.67 Å.

Introduction

Porous materials are crystalline or amorphous solids that permit the inclusion of small molecules through holes in their structures. These hollow structures are classified as nanoporous when the cavities are <15 Å in diameter and mesoporous for materials with cavities in the range 15–1000 Å. The applications of porous crystalline materials are diverse: from chemical separation based on size/shape effects to selective microenvironment for topochemical reactions; for optical resolution, asymmetric synthesis and catalysis; as technologically advanced materials in data imaging and storage, telecommunications, lasers, and ferromagnetism.[1] The natural and synthetic inorganic zeolites are the classical examples of nanoporous materials. The rigid but porous aluminosilicate lattice allows the diffusion of small guest molecules.[2]

The inclusion of guest molecules in the porous architecture of a crystalline host lattice produces binary adducts, which are referred to by different names depending on the chemical system, the application and/or the context—host–guest inclusion adducts, clathrates, molecular complexes, solvates, among others. In a recent paper, the definition of pseudopolymorphism has been expanded to cover all these closely related and yet distinct situations.[3] Pseudopolymorphs are solvated forms of a compound which have different crystal structures and/or differ in the nature of the included solvent. Studies towards host–guest structures are of increasing interest not only for their applications in materials science but also because they may be used as models for understanding drug–enzyme recognition and binding.

While the ability of microcrystalline zeolites to produce tetrahedral networks with cavities and channels of different sizes for various applications are well-known, recent synthetic studies have focussed on the design of highly ordered and regular porous structures with specific architecture and function.[4] In this respect, host frameworks with an organic core offer certain advantages. Structural diversity can be grafted in a pre-determined manner on the carbon skeleton through functional groups which can then be used through the intermediacy of supramolecular synthons[5] to control self-assembly in the solid-state. The inclusion and release of guest species is a much more facile process in organic hosts than in inorganic zeolites because the former adducts are usually assembled through co-crystallisation of the host and guest components. The entry of guest into zeolites usually requires pressure and their release takes place upon heating. For these reasons, and because of parallel developments in solid-state supramolecular synthesis,[6] the rational design and synthesis of organic microporous solids and host–guest materials is a current challenge in crystal engineering.[7]

Keywords: host–guest; hexagonal; triazine; halogen–halogen interaction; supramolecular synthon; hexachlorobenzene; 1,3,5-trinitrobenzene; hexamethylphosphoramide.

* Corresponding authors. Tel.: +91-40-3011338; fax: +91-40-3010567; e-mail: ansc@uohyd.ernet.in

0040–4020/00/$ - see front matter
PII: S0040-4020(00)00491-9

Within the broad area of organic porous lattices, channel-type inclusion host architectures are attractive because they produce a one-dimensional (1D) environment to probe a specific phenomenon or to manifest a particular property. Some common examples of channel-type organic inclusion hosts are trimesic acid, perhydrotriphenylene, urea, thiourea, cyclotriphosphazenes, tri-*o*-thymotide, cyclodextrins, and cyclic oligopeptides.[1,4] The construction of hexagonal lattice inclusion hosts (hexahosts) based on trigonal molecular scaffolds continues to elicit intense interest in current approaches.[8] The synthesis of polar inclusion crystals from dipolar components can be induced in the 1D channels of perhydrotriphenylene.[9] Carbon nanotubes,[10] a structural sub-class of fullerene, are stable hollow tubes made of graphite sheets rolled up in a helical fashion and capped at both ends with pentagons. Prepared in lengths of 1 μm or longer with an inner diameter ranging from 20 to 300 Å, carbon nanotubes are the strongest fibres known to date.

Recently we have reported the crystal structures of a series of inclusion compounds of hexahost 2,4,6-tris-4-(bromophenoxy)-1,3,5-triazine with hexachlorobenzene,

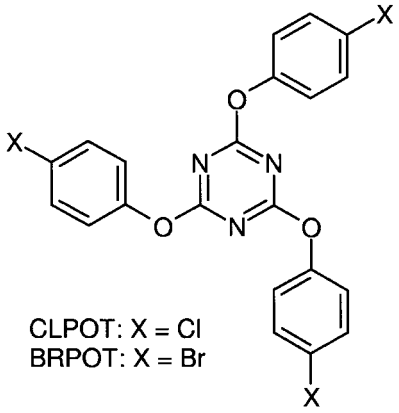

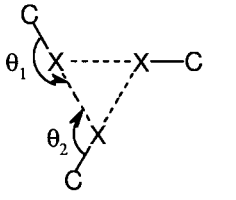

Cl_3 and Br_3 synthon

CLPOT.HCB (2:1)
CLPOT.HMB (2:1)
BRPOT.HMB (2:1)
CLPOT.TNB (2:1)
BRPOT.TNM (2:1)
CLPOT.HMPA (2:1)
BRPOT.HMPA.CA (2:4:1)

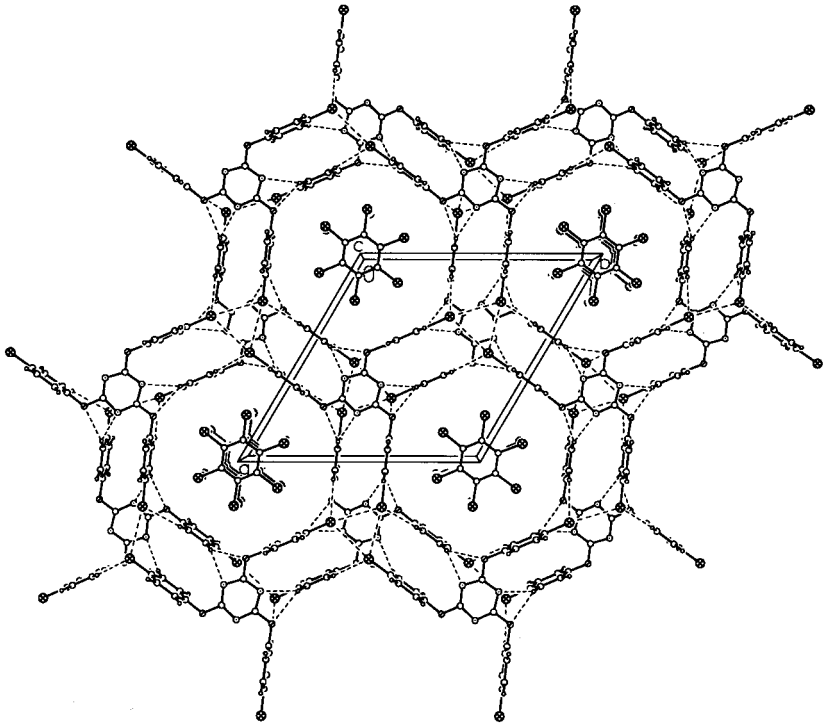

Figure 1. Crystal structure of CLPOT·HCB (2:1). View of the *ab*-layer to show the hexagonal arrangement of alternating triazine and Cl_3-trimer synthons. The HCB guest species is disordered along the channel axis.

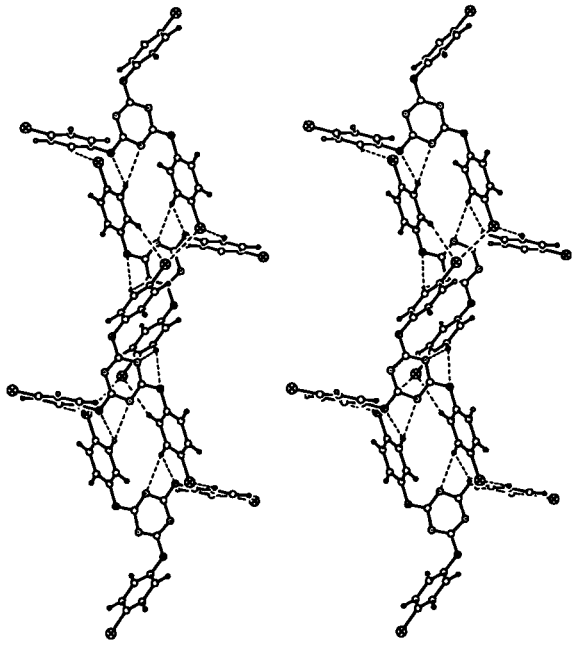

Figure 2. Stereoview of a side projection to show the host channel walls in CLPOT·HCB. Notice the profusion of phenyl C–H···O, C–H···N and C–H···Cl hydrogen bonds and the bifurcation at donor and acceptor groups. Channel walls in the BRPOT lattice have a similar architecture.

2,4,6-collidine, 1-methylnaphthalene and mesitylene guests.[11] The host molecules self-assemble via alternating triazine and Br···Br supramolecular synthons to produce a hexagonal array which extends in the third dimension to form channel walls through weak C–H···O, C–H···N and C–H···Br hydrogen bonding interactions. The honeycomb microporous architecture of bromo-triazine includes a variety of guest molecules of different size/shape, signifying robustness of the Br_3 trimer synthon during crystallisation. We report herein some inclusion crystal structures of 2,4,6-tris-4-(*chl*oro*p*hen*o*xy)-1,3,5-*t*riazine (CLPOT) and 2,4,6-tris-4-(*br*omo*p*hen*o*xy)-1,3,5-*t*riazine (BRPOT), thereby expanding the scope of our study to a family of closely related structures with Cl- and Br-substituted triazine hosts and a comparison of their inclusion properties with the same or similar guest. In this paper, six isomorphous inclusion compounds that crystallise in the space group $P6_3/m$, namely CLPOT·hexachlorobenzene (HCB), CLPOT·hexamethylbenzene (HMB), BRPOT·HMB, CLPOT·trinitrobenzene (TNB), BRPOT·trinitromesitylene (TNM) and CLPOT·hexamethylphosphoramide (HMPA), together with a ternary crystal belonging to the space group $R3c$, BRPOT·HMPA·cyanuric-acid (CA), are discussed.

Results and Discussion

CLPOT·HCB (2:1)

When a stoichiometric mixture of CLPOT and HCB was dissolved in benzene and a few drops of ethyl acetate added slowly to the solution, prism-like, colourless crystals precipitated within a few days which were characterised as the CLPOT·HCB (2:1) complex by X-ray diffraction in the space group $P6_3/m$. Both the triazine host and the HCB guest lie in the mirror plane. The asymmetric unit contains 1/6 triazine and 1/12 HCB to give an occupancy of 2 host and 1 guest molecules in the unit-cell. The triazine molecules occupy the $\bar{6}$ site at $z=1/4$ and self-assemble via the Cl···Cl (3.45 Å, $\theta_1=172.2°$, $\theta_2=112.2°$) supramolecular synthon to produce a hexagonal layer (Fig. 1). The Cl_3 trimer synthon aggregates through the polarisation-induced type II halogen($\delta+$)···halogen($\delta-$) interaction.[12] Because the polar $\delta(+)$ region of one halogen (along the C–X bond) approaches the equatorial $\delta(-)$ region of another halogen (almost perpendicular to the C–X bond) in a cyclic pattern, the trimer synthon is further stabilised by cooperativity. Thus, alternating molecular (triazine) and supramolecular (Cl_3) synthons with trigonal symmetry constitute the nodes of the lamellar honeycomb network while stacking of these synthons related by two-fold screw axis along the *c*-direction (at $z=1/4$, 3/4) leads to crystal growth in the third dimension. The phenyl rings are orthogonal to the *ab*-plane and form the channel walls through a profusion of C–H···O, C–H···N, C–H···Cl (2.6–3.0 Å, Table 2) hydrogen bonds[13] to complete the hexahost framework (Fig. 2). The HCB guest species are statistically disordered along the 1D infinite hexagonal channel and located alternately at $z=1/4$ and $z=1/2$ with $\bar{3}$ and $\bar{6}$ site-symmetry, respectively. In effect, a hexahost lattice is produced by the concerted stabilisation from numerous, though weak, hydrogen bonds and heteroatom interactions and shown to include guest molecules. Our strategy complements traditional approaches[1,4] wherein host frameworks have been constructed with conventional (strong O–H···O, N–H···O) hydrogen bonds.

The cross section of CLPOT·HCB channel is 105 $Å^2$. In contrast, the 2:1 molecular complex of BRPOT and HCB is layered with offset (space group $R\bar{3}$). The hexachlorobenzene molecule is ordered and sandwiched between two Br_3 synthons of neighbouring layers, being accommodated in a cavity of cross-sectional area 103 $Å^2$.[11] Crystallographic data of the crystal structures in this study are summarised in Table 1 and the geometries of intermolecular interactions are listed in Table 2.

CLPOT·HMB and BRPOT·HMB (2:1 each)

These two crystal structures are isomorphous (space group $P6_3/m$) and include disordered guest molecules in their porous channels of cross-sectional area 104 and 107 $Å^2$, respectively. The phenoxy rings in the slightly smaller framework of CLPOT are orientationally disordered over two sites with a dihedral angle of 24.9° to accommodate the HMB guest while they are ordered for the BRPOT host. Disordered HMB molecules in the ordered, hexagonal channels of BRPOT are displayed in Fig. 3. The disorder of phenoxy moiety was noted earlier in the collidine and mesitylene clathrates of BRPOT,[11] the reason being the larger guest size compared to pore area of the host lattice (104 $Å^2$). The van der Waals diameter of triazine lattice (12–13 Å) and other channel-type hosts are all in the nanometer scale: trimesic acid (14–15 Å), urea and thiourea (5–7 Å), perhydrotriphenylene (5–6 Å), cyclotriphosphazenes (9–10 Å), cyclodextrins (5–9 Å) and cyclic oligopeptides (7–13 Å).

Table 1. Crystallographic data for clathrates in this study

	CLPOT·HCB	CLPOT·HMB	BRPOT·HMB	CLPOT·TNB	BRPOT·TNM	CLPOT·HMPA	BRPOT·HMPA·CA
Empirical formula	$(C_{21}H_{12}Cl_3N_3O_3)$ $(C_6Cl_6)_{0.5}$	$(C_{21}H_{12}Cl_3N_3O_3)$ $(C_{12}H_{18})_{0.5}$	$(C_{21}H_{12}Br_3N_3O_3)$ $(C_{12}H_{18})_{0.5}$	$(C_{21}H_{12}Cl_3N_3O_3)$ $(C_6H_3N_3O_6)_{0.5}$	$(C_{21}H_{12}Br_3N_3O_3)$ $(C_9H_9N_3O_6)_{0.5}$	$(C_{21}H_{12}Cl_3N_3O_3)$ $(C_6H_{18}N_3PO)_{0.5}$	$(C_{21}H_{12}Br_3N_3O_3)$ $(C_6H_{18}N_3PO)_{2.0}$ $(C_3H_3N_3O_3)_{0.5}$
Formula wt.	603.07	541.82	675.20	567.24	721.66	550.29	1017.01
Crystal habit	colourless prism	colourless prism	colourless block	yellow prism	colourless prism	yellow prism	colourless prism
Size (mm^3)	0.40×0.45×0.50	0.30×0.30×0.45	0.30×0.40×0.50	0.25×0.30×0.50	0.30×0.35×0.42	0.30×0.40×0.50	0.40×0.40×0.52
Crystal system	hexagonal	hexagonal	hexagonal	hexagonal	Hexagonal	Hexagonal	hexagonal
Space group	$P6_3/m$ (No. 176)	$P6_3/m$ (No. 176)	$P6_3/m$ (No. 176)	$P6_3/m$ (No. 176)	$P6_3/m$ (No. 176)	$P6_3/m$(No. 176)	$R3c$ (No. 161)
a (Å)	15.435(2)	15.411(2)	15.554(4)	15.255(2)	15.719(2)	15.234(2)	15.615(2)
b (Å)	15.435(2)	15.411(2)	15.554(4)	15.255(2)	15.719(2)	15.234(2)	15.615(2)
c (Å)	6.876(1)	6.867(1)	6.951(3)	7.005(2)	7.034(1)	6.880(1)	63.670(1)
α (deg)	90	90	90	90	90	90	90
β (deg)	90	90	90	90	90	90	90
γ (deg)	120	120	120	120	120	120	120
Z	2	2	2	2	2	2	6
V $(Å)^3$	1418.7(4)	1412.4(4)	1456.4(8)	1411.6(4)	1505.2(4)	1382.8(4)	13445(3)
D_{calc} (Mg/m^3)	1.412	1.274	1.540	1.335	1.592	1.322	1.507
F (000)	606	558	666	576	708	566	6204
2θ range	3–50	3–52	3–56	3–52	3–52	3–55	3–52
Index ranges	(0, 0, 0)~(15, 15, 8)	(0, 0, -7)~(15, 15, 8)	(-20, -20, -9)~(19, 13, 9)	(-1, -19, -1)~(17, 1, 9)	(0, -18, -8)~(19, 16, 8)	(0, 0, 0)~(17, 17, 18)	(-18, -17, -77)~(18, 18, 27)
M.p. (°C)	230–231	209–210	232–234	209–210	219–221	209–210	240–242
Data collection	Rigaku AFC7R	Rigaku RAXIS IIC	Bruker SMART	Siemens P4	Rigaku RAXIS IIC	Rigaku AFC7R	Rigaku RAXIS IIC
$R1$	0.0745	0.0771	0.0678	0.0564	0.0687	0.0456	0.0606
W$R2$	0.2085	0.1876	0.1431	0.1236	0.1803	0.1232	0.1579
GOF	1.023	1.239	0.876	0.991	1.276	1.002	1.098
N-total[a]	992	1452	7912	2980	4452	1274	12047
N-indep[b]	890	843	1283	1155	977	1151	3513
N-obsd[c]	630	750	761	682	916	788	3340
Variables	115	115	97	379	107	123	341
C_k[d]	0.76	0.81	0.75	0.69	0.76	0.81	0.75

[a] N-total is the total number of reflections collected
[b] N-indep is the number of independent reflections
[c] N-obsd is the number observed reflections based on the criterion $I>2\sigma$ (I)
[d] C_k is the packing fraction calculated using PLATON program

Table 2. Geometrical parameters of host–host, host–guest and guest–guest intermolecular interactions in complexes

Complex	Interaction[a]	d, Å	D, Å	θ, deg	Type
CLPOT·HCB	C(3)–H···Cl	2.97	3.921(7)	146.5	Host–host
	C(4)–H··· N	2.67	3.616(5)	145.3	Host–host
	C(4)–H···O	2.82	3.738(6)	142.9	Host–host
	Cl···Cl		3.454(2)	172.2/112.2	Host–host
CLPOT·HMB	Cl···Cl		3.477(2)	171.5/111.5	Host–host
BRPOT·HMB	C(3)–H···Br	2.94	3.903(5)	148.3	Host–host
	C(4)–H···N	2.85	3.768(7)	143.0	Host–host
	C(4)–H···O	2.92	3.862(8)	145.7	Host–host
	Br···Br		3.472(18)	111.7/171.7	Host–host
CLPOT·TNB	C(3)–H···Cl	2.93	3.891(3)	148.7	Host–host
	C(4)–H···O	2.75	3.696(3)	146.2	Host–host
	C(4)–H···N	2.72	3.648(4)	144.1	Host–host
	C(1)-O···O		3.167(9)	148.2	Host–guest
	N(2)-O···O		3.167(9)	178.4	Guest–host
	N(2)-O···Cl		3.536(9)	161.4	Guest–host
	Cl···Cl		3.419(16)	170.6/110.6	Host–host
	$\pi\cdots\pi$		3.502		Guest–guest
BRPOT·TNM	C(3)–H···Br	2.99	3.954(7)	148.9	Host–host
	C(4)–H···N	2.88	3.812(9)	143.6	Host–host
	C(4)–H···O	2.98	3.911(8)	143.9	Host–host
	Br···Br		3.498(14)	171.8/111.8	Host–host
CLPOT·HMPA	Cl···Cl		3.444(8)	169.5/109.5	Host–host
BRPOT·	N(3)–H···O	1.71	2.709(9)	168.9	Guest–guest
HMPA·CA	C(10)–H···O	2.48	3.519(11)	161.5	Host–guest
	C(11)–H···O	2.69	3.527(12)	133.5	Host–guest
	C(13)–H···N	2.77	3.808(12)	161.2	Host–host
	C(6)–H···N	2.77	3.811(12)	161.1	Host–host
	C(6)–H···O	2.87	3.761(12)	140.0	Host–host
	C(16)–H···O	2.79	3.721(16)	144.5	Guest–guest
	C(18)–H···O	2.49	3.305(13)	131.1	Guest–guest
	C(3)–H···O	2.39	3.447(11)	165.8	Host–guest
	C(20)–H···O	2.53	3.476(16)	145.1	Guest–guest
	C(7)–H···Br	3.07	4.001(9)	144.6	Guest–host
	C(14)–H···Br	3.25	4.124(9)	138.7	Host–host
	Br···Br		3.851(17)	169.0/110.7	Host–host
	Br···Br		4.039(2)	169.5/110.8	Host–host

[a] C–H and N–H distances are neutron-normalised

The disorder of HMB in both CLPOT and BRPOT channels is similar to that of HCB in its CLPOT complex, that is HMB is located at z=1/4 and z=1/2 with $\bar{3}$ and $\bar{6}$ site-symmetry, respectively. In this context, a comparison of the volume of Cl and Me groups (20 and 24 Å^3) is pertinent. The basis for the so-called chloro–methyl exchange rule[14]—crystal structures in which a methyl group is replaced by a chloro group are isostructural/isomorphous—is the similar van der Waals volume of these two groups. It may further be noted that while crystal structures of pure HCB and pure HMB are very different and that they do not obey the chloro–methyl exchange rule, the above

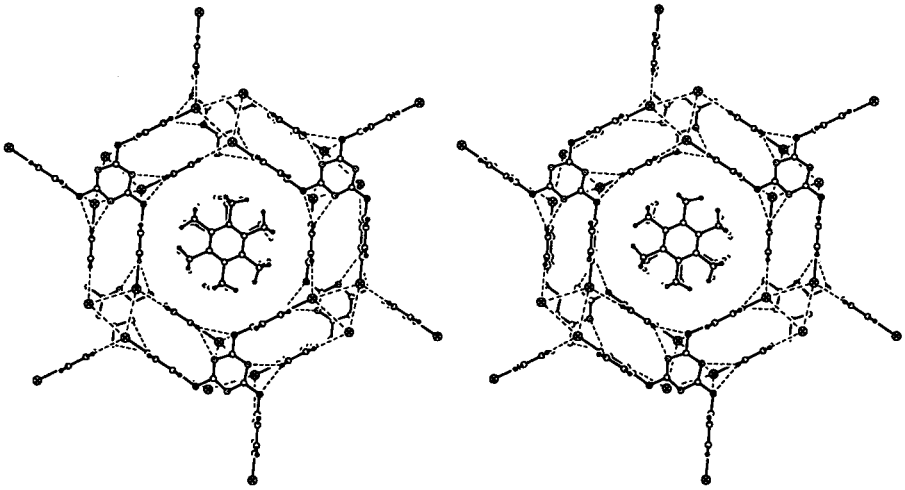

Figure 3. Crystal structure of BRPOT·HMB (2:1). Stereoview of the *ab*-layer to show the hexahost framework and the disordered HMB guest species along the porous channel.

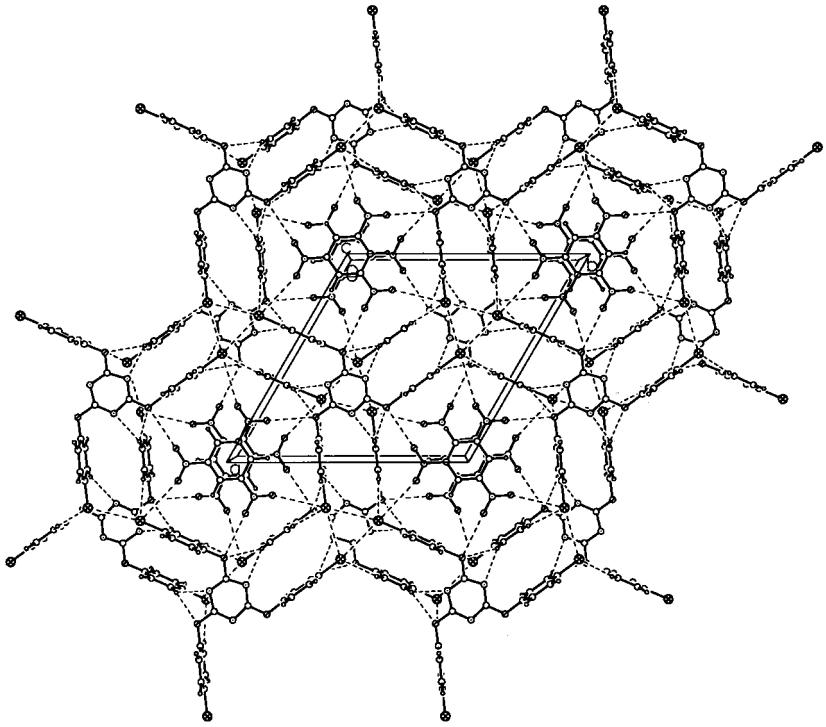

Figure 4. Crystal structure of CLPOT·TNB (2:1). The guest species are ordered in the hexagonal channel. Notice the O···O and O···Cl interactions between nitro groups of the guest and heteroatoms of the host lattice.

examples show that when these molecules are constrained in 1D channels, their structural role is quite similar and is in contrast to the behaviour exhibited in their respective single-component crystals.

CLPOT·TNB and BRPOT·TNM (2:1 each)

1,3,5-Trinitrobenzene is an archetypical component in molecular complexes and host–guest inclusion compounds. Because of its electron-deficient aromatic ring TNB readily forms charge–transfer complexes with aromatic hydrocarbons. The profusion of acceptor O-atoms results in molecular complexes with hydrogen bond donor molecules. It was reasoned that the trigonal symmetry of TNB and its size-similarity with HCB/HMB should make it a suitable guest molecule for this study. A solution of TNB and CLPOT in benzene was carefully layered with a few drops of ethyl acetate to obtain single crystals.

In CLPOT·TNB ($P6_3/m$), there is a hexagonal network of alternating triazine (molecular) and Cl_3 (supramolecular) synthons at $\bar{6}$ sites with the nanoporous channels filled with ordered TNB molecules located at $z=1/4$ and $z=3/4$ and stacked in a staggered configuration within each channel (Fig. 4). The ordered orientation of TNB cannot be reliably ascribed to specific hydrogen bond(s)[13] and/or to (nitro)O···Cl(triazine) interactions[15] because many of the host–guest contacts are long and bent (Table 2). It is likely that numerous weak interactions together with the match of trigonal symmetry between guest and host are sufficient to stabilise the fully ordered arrangement in the crystal.

The TNB molecules, related by a $6_3/m$ axis, are stacked in the channel at a separation of $c/2=3.50$ Å, shown as a stereoview in Fig. 5. The π-stacking of TNB molecules at such close separation without parallel offset is unprecedented. A search of the Cambridge Structural Database[16] (CSD, 2,07,507 entries, version 5.18, October 1999 update) showed that this is the only crystal structure in which two TNB molecules are π-stacked at a distance about the sum of their van der Waals radii (3.4 Å). Other examples in the CSD of organic, neutral, molecules with a 1,3,5-trinitrophenyl sub-structure have longer inter-centroid π···π separation: JAPKIU (3.88 Å), JUPRIV (3.85 Å), MPICIN (3.58 Å), NAWQAD (3.90 Å) and TAFCEI (3.53 Å). While there are examples of aromatic hydrocarbon crystal structures in which C···C distances are <3.4 Å,[17a] stacking of TNB molecules at 3.50 Å intermolecular separation in the present case is better explained through mechanisms proposed for electron-deficient aromatic rings.[17b,c] A yet another unusual attribute of TNB in the CLPOT cage is the perfectly planar arrangement of the aromatic ring together with the three NO_2 groups. The only other crystal structure in which TNB is present in the all-planar conformation is in its layered 1:1 complex with trimethyl isocyanurate (space group $P\bar{6}$).[18] The π-stacking of TNB molecules at such short internuclear separation in the high energy all-planar conformation is unique, and could be a result of the guest being constrained in a narrow channel.

The fact that TNB is ordered suggests that guest–size and host–channel area are perfectly matched with these two components. Based on our observations with the HMB solvate regarding order and disorder of phenoxy moiety in BRPOT and CLPOT, respectively, it was reasoned that the BRPOT channel is too large to include TNB. Indeed, several

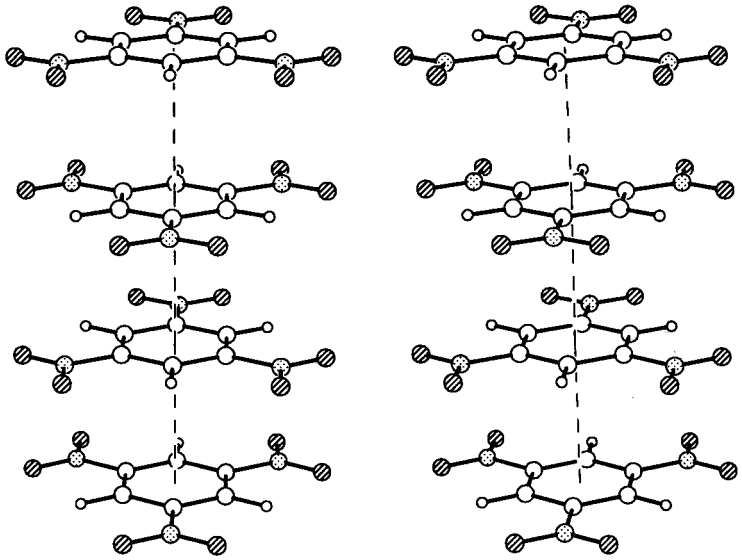

Figure 5. Stereoview of TNB guests in the 1D channels of CLPOT (host not shown). Notice the perfectly planar TNB molecule and the parallel stacking without offset of 6_3-related molecules at 3.50 Å separation. Such an arrangement of TNB molecules is unique in the CSD.

attempts to obtain BRPOT·TNB co-crystals were futile. However, and as anticipated, the bigger TNM guest was trapped in the porous architecture of BRPOT in a 2:1 host–guest ratio. These inclusion crystals are isomorphous ($P6_3/m$) and TNM is statistically disordered. The host phenoxy groups are ordered suggesting a size complementarity between guest and host. Finally we note that no CLPOT·TNM co-crystals could be obtained after several attempts. All these experiments give an idea of the extent to which the host framework is adaptive towards inclusion of guest species and also of situations in which no adduct crystals are formed.

CLPOT·HMPA (2:1) and BRPOT·HMPA·CA (2:4:1)

Recrystallisation of CLPOT from HMPA afforded crystals of the isomorphous solvate ($P6_3/m$). In this structure, both host and guest molecules are disordered: HMPA is three-fold disordered and phenoxy groups of triazine are disordered over three orientations (Fig. 6).

In contrast to the normal structure of CLPOT·HMPA, recrystallisation of BRPOT from HMPA did not provide a binary adduct. Instead, a ternary host–guest–guest complex of BRPOT, HMPA and cyanuric acid (CA) in 2:4:1

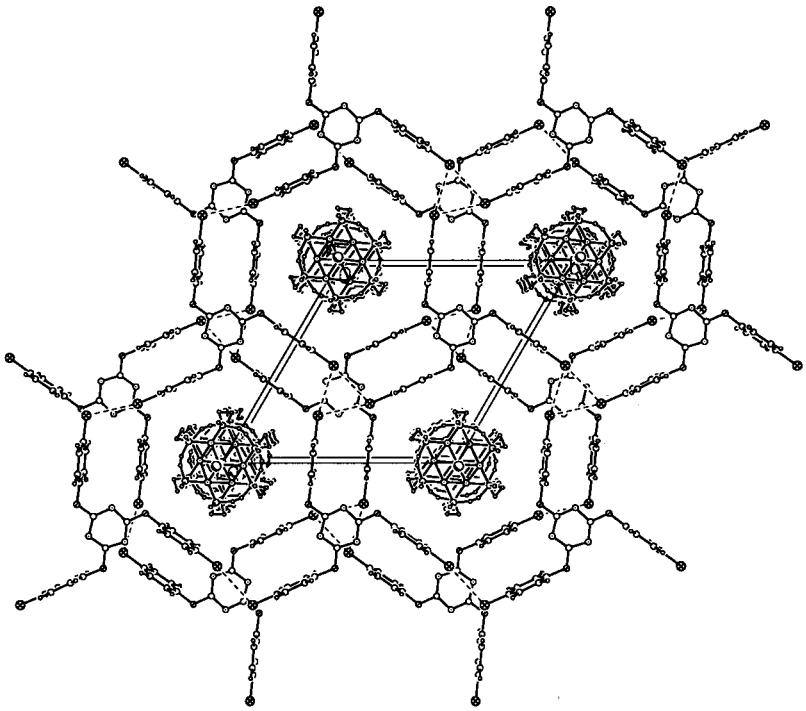

Figure 6. Crystal structure of CLPOT·HMPA (2:1). Guest molecules are disordered in the hexagonal channels of host. Only one orientation of the disordered phenoxy moiety is shown.

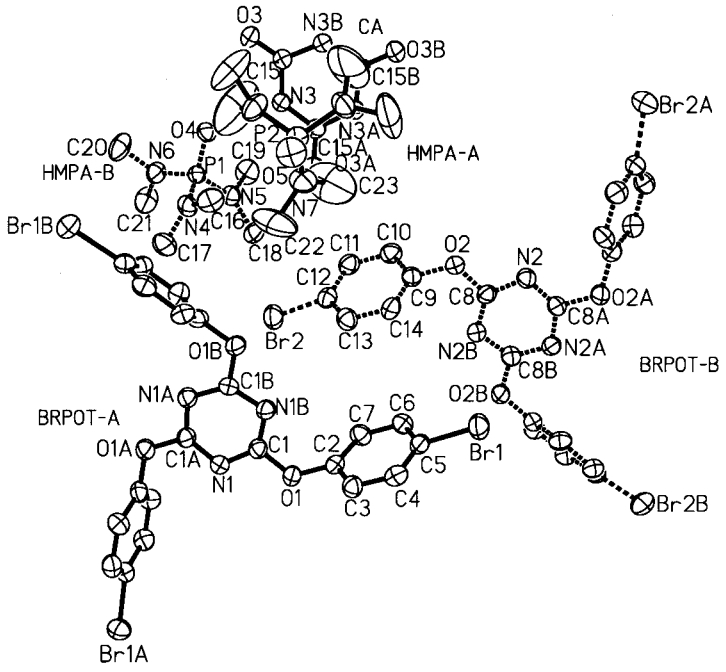

Figure 7. Perspective ORTEP drawing of BRPOT·HMPA·CA (2:4:1) showing two independent BRPOT molecules (A, B), two independent HMPA molecules (A, B) and CA. Symmetry-independent molecules are shown with solid and dotted lines.

stoichiometry was obtained as determined by X-ray crystallography. The asymmetric unit (Fig. 7) contains two independent BRPOT molecules in a similar conformation (A and B, both located on 3-fold screw axis), two independent HMPA molecules (A lying on 3-fold axis; B occupying general position), and CA (at a 3-fold symmetry site). The structure was solved and refined in the space group $R3c$ based on a hexagonal unit cell with obverse setting ($a=b=15.61$ and $c=63.67$ Å).

Two independent BRPOT molecules constitute a double-layer that resembles the host lattice in the aforementioned $P6_3/m$ complexes with triazine and Br···Br synthons (3.85, 4.04 Å, $\theta_1=169.0, 169.5°$ and $\theta_2=110.7, 110.8°$). However, instead of generating a channel structure, the double-layers are arranged in a staggered configuration along the c-axis, thus forming hexagonal cavities. The phenoxy groups of triazine are tilted with respect to the ab-plane (66.0 and 76.4°) and grow inwards to form a concave, cage-like dome with C–H···O, C–H···N and C–H···Br hydrogen bonds[13] (Table 2). The solvated HMPA(A) molecule is trapped in this bowl-shaped cavity with its P═O group oriented parallel to the c-axis (Fig. 8). Each CA molecule is connected to three HMPA(B) molecules through N_{CA}–H···O_{HMPA} hydrogen bonding, generating an additional layer running parallel to and sandwiched between BRPOT

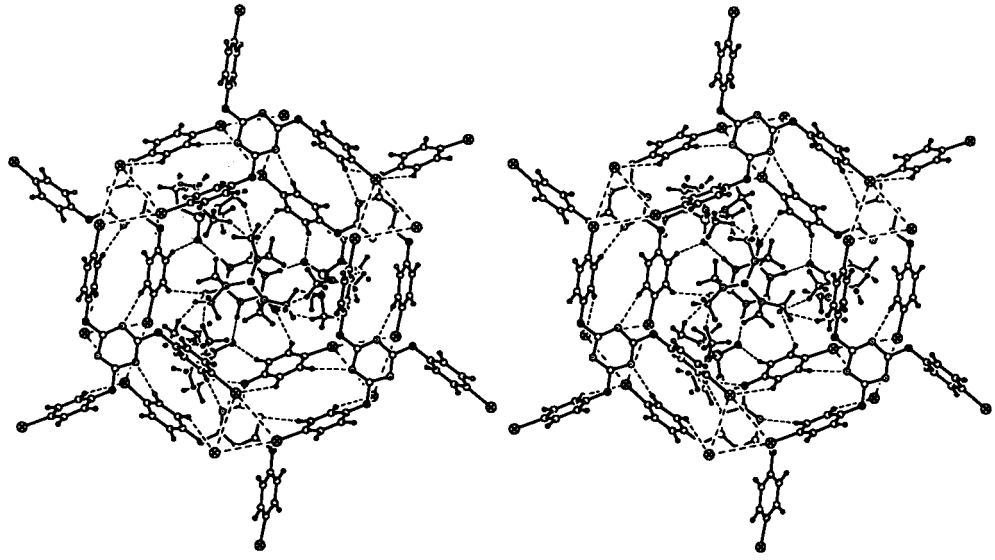

Figure 8. Stereoview of the bowl-shaped structure down the c-axis in BRPOT·HMPA·CA. The walls of the bowl are constructed with triazine phenoxy groups and the hollow region is filled with guest molecules. Notice the profusion of host–host, guest–guest and host–guest hydrogen bonds. Both host and guest species are fully ordered in the crystal.

double-layers, in which CA molecules are stacked with triazine host at a separation of 3.98 Å. To avoid steric crowding, the phenoxy groups of BRPOT and HMPA(B) molecules are staggered with respect to one another. Interestingly, the host and the guest molecules are fully ordered, except the terminal methyl groups of HMPA(A), and connected through an intricate network of host–host, guest–guest and host–guest hydrogen bonds. The N–H donor of CA is bonded to the O-atom (1.71 Å, 168.9°) of HMPA(B) while the carbonyl O-atom of CA is C–H···O bonded with donor groups of triazine phenoxy (2.69 Å, 133.5°) and HMPA(B) molecules (2.79, 2.49 Å, 144.5, 131.1°) in a trifurcated motif. The P═O group of HMPA(A) along the *c*-axis is bonded to the *N*-methyl donor of HMPA(B) on the periphery of the channel (2.53 Å, 145.1°). The P═O acceptor group of HMPA(B) is bonded strongly to phenoxy C–H donor of triazine (2.48 Å, 161.5°). In summary, the ternary crystal structure illustrates many interesting features: host and guest molecules are connected through numerous weak hydrogen bonds; all components are ordered in the crystal lattice; and most significantly, the guest molecules act as a template for self-assembly of the host framework. Indeed, a crystal is a supermolecule par excellence.[19]

It may be noted that while *a*- and *b*-axes of the hexagonal cell of BRPOT·HMPA·CA are nearly equal to other isomorphous crystals (15–16 Å), the *c*-axis (63.67 Å) is 9 times the repeat distance of triazine host (∽7 Å). The bigger unit cell in the ternary clathrate results from the alternating, staggered arrangement of BRPOT double-layers and CA-HMPA(B) layer, shown in Fig. 9. The asymmetric array of host and guest molecules along the *c*-axis (up to down) is: CA-HMPA(B), triazine of BRPOT(A), Br_3 synthon of BRPOT(B), CA-HMPA(B), Br_3 synthon of BRPOT(A), triazine of BRPOT(B), CA-HMPA(B), HMPA(A). The *c*-glide related stack completes the unit cell. This accounts for the super-cell structure of the ternary complex containing 12 host and 30 guest molecules.[20] Because of the unusually long *c*-axis, the encapsulated structure resembles a cylindrical medicine-capsule[21] filled with guest molecules: CA-HMPA(B) complex is the hydrogen bonded base and the inverted HMPA(A) molecule is the hydrophobic cap. However, instead of the capsule being closed with its inversion-related partner, successive units are aligned parallel and in one direction, resulting in a polar arrangement of molecules (Fig. 10a). The polar packing in this ternary crystal may be compared with the crystal structure of a fullerene-shaped hydrocarbon reported recently ($C_{36}H_{12}$, space group *R*3*c*)[22] in which the bowl-shaped hydrocarbon molecules are stacked on top of one another and furthermore all the stacks are aligned in one direction (Fig. 10b).

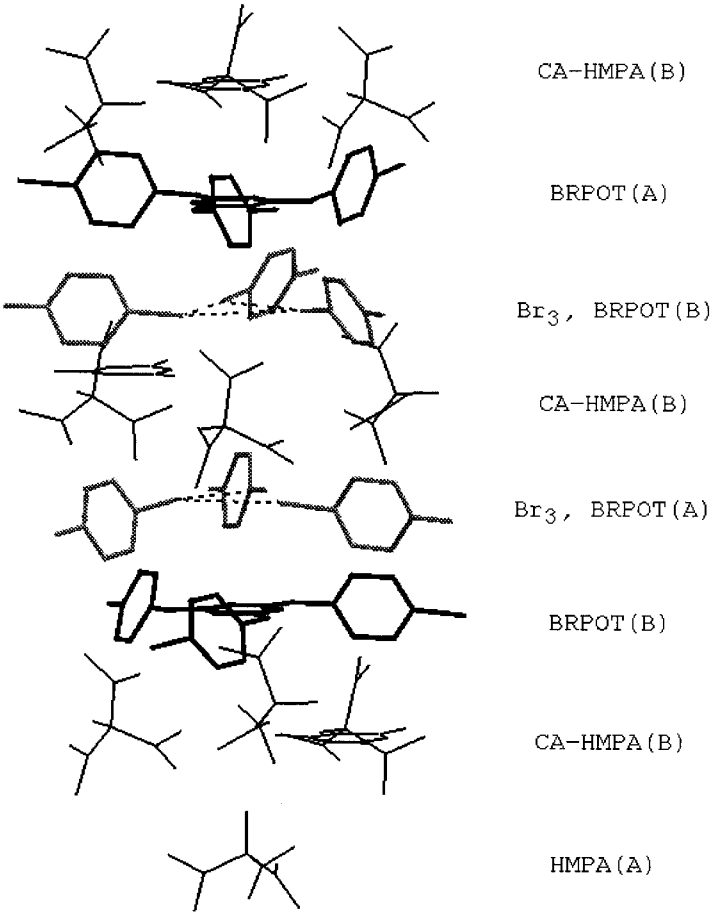

Figure 9. Stacking of host and guest components in BRPOT·HMPA·CA (*c*=63.67 Å). In the medicine-capsule-shaped cylindrical architecture (up to down), CA-HMPA(B) form the base, triazine and phenoxy moieties are the walls, and HMPA(A) molecule with its P═O pointing upward is the cap. Molecules are truncated for clarity.

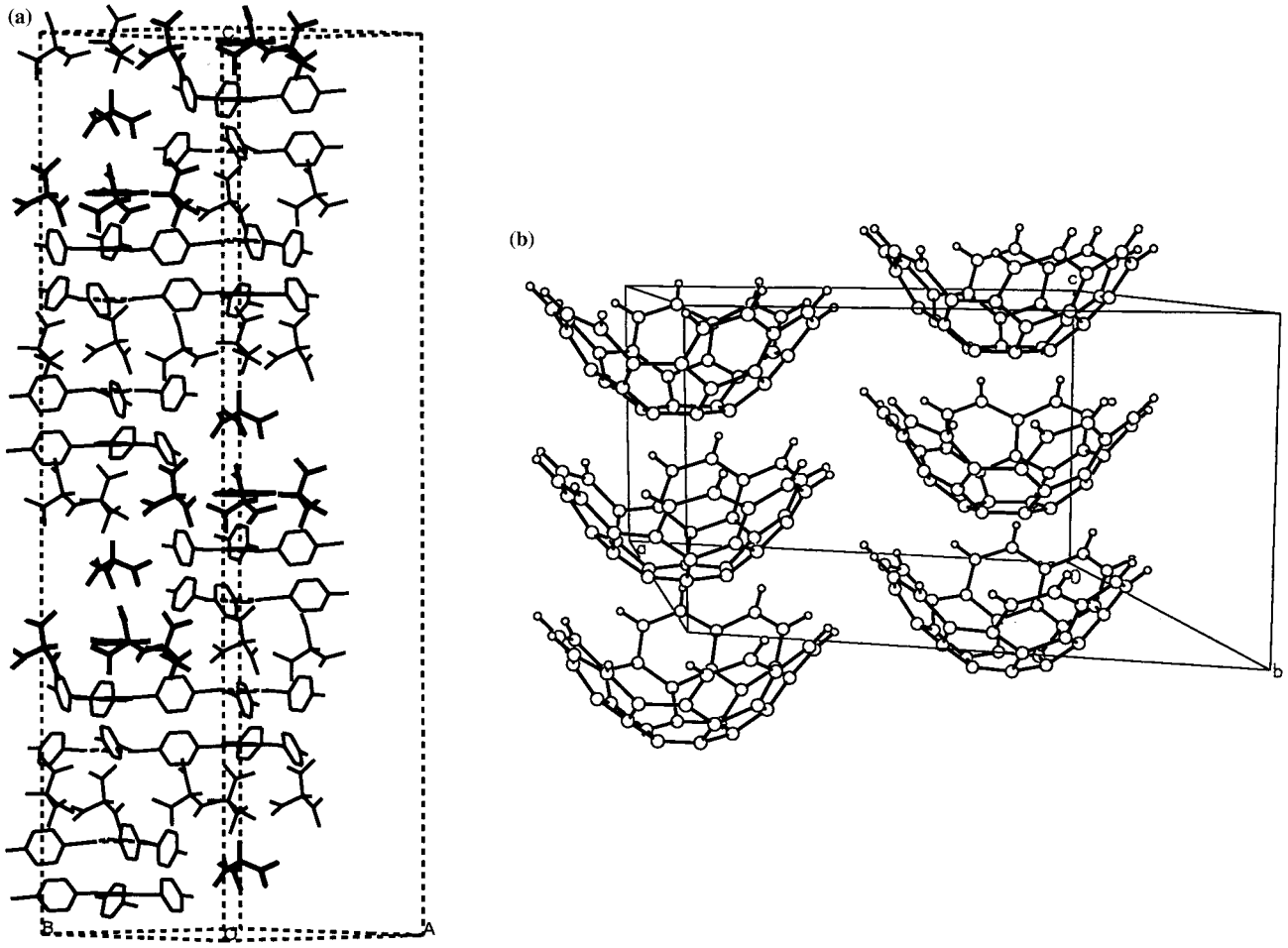

Figure 10. Polar stacking of glide-related units in BRPOT·HMPA·CA (a) and $C_{36}H_{12}$ (b, Ref. 22). Both the structures are in *R*3*c* space group. Molecules at the base and cap in (a) are highlighted in bold to show the capsule outline.

The ternary complex BRPOT·HMPA·CA (2:4:1) has many notable features. (1) While binary host–guest adducts abound, the isolation of a three-component complex is a rare phenomenon,[23] and is usually fortuitous. Our serendipitous result is noteworthy in the category of ternary crystals because the two guest species have very different size, shape and hydrogen bonding properties. (2) The ordered orientation of the three components in the crystal and the intricate network of N–H···O, C–H···O, C–H···N and C–H···Br hydrogen bonds highlights the structural role of these interactions. Weaker than conventional hydrogen bonds, the concerted energy contribution from the numerous C–H···O/N/Br interactions is sufficient to overcome entropic effects. (3) The multiple hydrogen bonding capability of HMPA is exemplified through the (B) molecules which act simultaneously as donors and acceptors. The last of these points is closely related to a recent Cambridge Database study on the probabilities of solvent inclusion in crystals,[24] and is elaborated next.

The rationale for solvent-inclusion in molecular crystals has been identified as the ability of that particular solvent to behave both as a donor and as an acceptor of hydrogen bonds, in other words, to the intermediacy of multi-point recognition supramolecular synthons during crystallisation. For example, DMF (dimethyl formamide) is the top solvent based on its frequency of occurrence[24] because it can accept O–H, N–H and C–H hydrogen bonds and also donate a C–H···O bond through its *N*-methyl group to the same or another molecule (Fig. 11a). The similarity of HMPA with DMF is obvious as the P═O group of HMPA is a very strong acceptor and the *N*-methyl are C–H donors. The supramolecular synthons in HMPA solvates as retrieved from the CSD are displayed in Fig. 11b. Since the number of HMPA pseudopolymorphs is small (15), the data are not statistically significant but the trends and similarity with DMF are amply clear.

In the present pair of co-crystals it is noted that while both CLPOT and BRPOT were recrystallised from HMPA under identical conditions, the former structure is a binary complex (with HMPA) while the latter includes HMPA and CA guests. In order to understand these differences, CLPOT and BRPOT were recrystallised from HMPA in control experiments with stoichiometric amount of CA added. Interestingly, BRPOT gave the same ternary crystals as confirmed by X-ray diffraction but in case of CLPOT a binary adduct was obtained. In the crystallisation experiments, hydrolysis of *para*-halophenoxy-triazine by adventitious water will produce cyanuric acid in situ during slow evaporation of solvent over 2–3 days. A plausible explanation for obtaining the ternary complex with BRPOT could

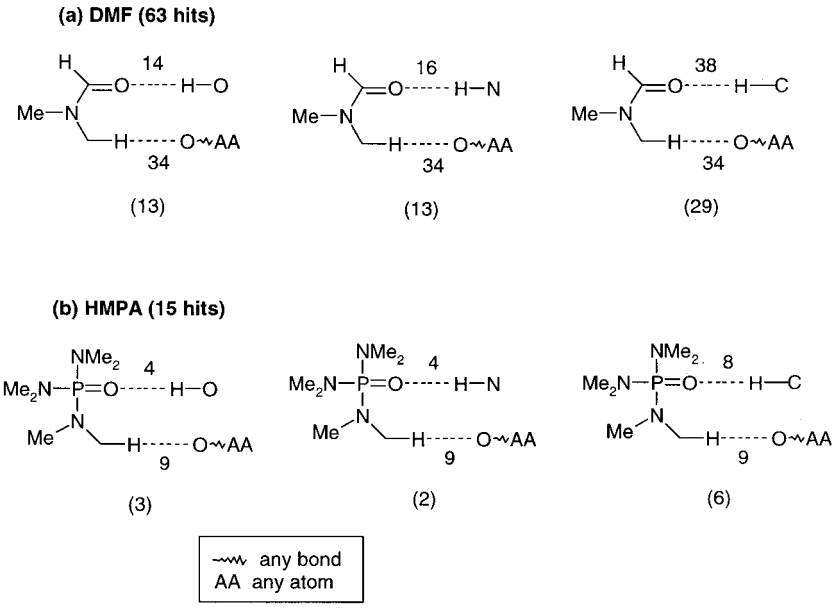

Figure 11. Frequency of single- and multi-point hydrogen bonded supramolecular synthons in solvates of DMF (a, Ref. 24) and HMPA (b, this study). Numbers in parentheses are hits with two-point recognition. Geometric criteria applied: O/N–H···O 1.5<d<2.2 Å, 140<θ<180°; C–H···O 2.0<d<3.0 Å, 110<θ<180°. H-atom positions neutron-normalised: O–H 0.983, N–H 1.009, C–H 1.083 Å.

be that its porous cavity is of the correct size to include CA while the channel in CLPOT is slightly smaller to include this guest. This is borne out by independent experiments with added CA.

Conclusions

A synthesis, be it molecular or supramolecular, has a target and a strategy.[25] The supramolecular target in this study is the hexagonal network. The strategy employed to rationally assemble the hexahost is a knowledge of the halogen–halogen interactions (X···X) and the importance of symmetry (C_3 molecule). The designed match of trigonal symmetry at molecular (triazine) and supramolecular (X_3 synthon) nodes steers crystallisation in a predictable manner. At a functional level, guest inclusion is facile and competing interpenetration is not a complication in the porous lattice of triazine.

We have shown the generality of a new, hexagonal host scaffold assembled with weak hydrogen bonds and hetero-atom interactions. Retrosynthesis through supramolecular synthons and the principles of non-covalent self-assembly are profitably exploited in this study. Structural control is achieved through a non-intersecting dissection of the three-dimensional (3D) architecture into two-dimensional (2D) layers and 1D channels together with interaction-insulation in the two domains. Efforts are ongoing to induce crystallisation in polar space groups for materials application of the tailored microenvironment.

Many of the guest molecules selected in this study are somewhat rare as adduct crystals in the CSD: HCB (0), HMB (10), TNB (38), TNM (0), HMPA (14) and CA (5). Further, these guest molecules exhibit interesting and unusual structural behaviour when constrained in 1D channels, as exemplified by HCB/HMB and TNB. The multi-point hydrogen bonding recognition of HMPA in the ternary crystal has implications in pseudopolymorphism.

Experimental Section

Synthesis

The title triazines were synthesised by condensation of cyanuric chloride with 4-halo-phenol as described earlier.[26]

2,4,6-Tris-(4-halo-phenoxy)-1,3,5-triazine. Cyanuric acid (10 mmol) was added to 4-halo-phenol (35 mmol) and the mixture heated at 200°C for 5 h. Upon cooling, the crude residue was extracted with boiling EtOH and recrystallised with $CHCl_3$ to give the pure product in 90% yield. Both compounds showed satisfactory NMR and IR spectra.

2,4,6-Tris-(4-chlorophenoxy)-1,3,5-triazine. ^{1}H NMR ($CDCl_3$, 200 MHz) δ 7.05 (*d*, *J*=8 Hz, 6H), 7.35 (*d*, *J*=8 Hz, 6H). IR (KBr) 3094, 3065, 1601, 1568, 1487, 1379, 1209 cm^{-1}.

2,4,6-Tris-(4-bromophenoxy)-1,3,5-triazine. ^{1}H NMR ($CDCl_3$, 200 MHz) δ 7.00 (*d*, *J*=6 Hz, 6H), 7.45 (*d*, *J*=6 Hz, 6H). IR (KBr) 3088, 3063, 1595, 1566, 1484, 1380, 1208 cm^{-1}.

Crystallisation

Crystallisation of the complexes was carried out at room temperature by dissolving equimolar amounts of CLPOT/BRPOT and the solid/liquid guest species (HCB, HMB, TNB, TNM) in benzene and then layering the solution slowly with ethyl acetate. Slow evaporation over a few days produced single crystals suitable for X-ray analysis. The HMPA solvates were obtained by recrystallisation of

CLPOT/BRPOT from the solvent at room temperature over a few days. In the experiments with added cyanuric acid, stoichiometric amounts of CLPOT/BRPOT and CA were dissolved in HMPA and the solvent allowed to evaporate slowly for obtaining single crystals. All crystals were found to be stable for weeks under ambient conditions. The size, shape and colour of crystals are summarised in Table 1.

X-Ray crystallography

Intensities were collected on a Rigaku AFC7R, Rigaku RAXIS IIC or Siemens P4 diffractometer using Mo-Kα radiation (λ=0.71073 Å) at 293(2) K. Empirical absorption corrections using ABSCOR (RAXIS data), ψ-scan (AFC7R data) or SADABS (P4 data) were applied.[27] Structure solution and refinement were performed with SHELXS-97 and SHELXL-97 program packages.[28] The partial occupancy of guest atoms were fixed differently during the refinement cycles so as to obtain good match between observed and calculated electron densities and acceptable *R* factors. The hydrogen atoms of triazine phenoxy groups and guest molecules (TNB, HMPA) were generated with idealised geometries and isotropically refined using Riding model. Refinement of coordinates and anisotropic thermal parameters of non-hydrogen atoms were carried out by full-matrix least-squares method. The crystallographic parameters and final *R* indices of all crystal structures are listed in Table 1.

Cambridge structural database

The recent update of CSD (October 1999, version 5.18, 207 507 entries)[16] was searched for organic structures (screen 57) with $R \leq 0.10$ (screen 88). Duplicate hits were removed manually. The geometric criteria applied for generating the hydrogen bond motifs of HMPA are: O–H···O, N–H···O $1.5<d<2.2$ Å, $140<\theta<180°$; C–H···O $2.0<d<3.0$ Å, $110<\theta<180°$. All H-atom positions were neutron-normalised (O–H 0.983, N–H 1.009, C–H 1.083 Å) for the intermolecular contacts in the CSD study and for the hydrogen bond geometries listed in Table 2. Since the number of HMPA hits is small (15), the additional screens applied for DMF in Ref. 24 (33, error-free; 35, no disorder; 85, chemical/crystallographic connectivity match; and 153, atom coordinates present) were not turned ON.

Acknowledgements

This research was funded by the Department of Science and Technology, Government of India (Project No. SP/S1/G29/98) and the Hong Kong Research Grants Council Earmarked Grant (Ref. No. CUHK 4206/99P). RKRJ and PKT thank DST and CSIR for fellowship support. We thank Prof. G. R. Desiraju for discussion and for bringing to our attention this topical theme issue of Tetrahedron.

References

1. (a) *Comprehensive Supramolecular Chemistry*; *Solid-state Supramolecular Chemistry: Crystal Engineering*; MacNicol, D. D., Toda, F., Bishop, R., Eds.; Pergamon Press: Oxford, 1996; Vol. 6. (b) Desiraju, G. R. *Curr. Opin. Solid State Mater. Sci.* **1997**, *2*, 451–454. (c) Langley, P. J.; Hulliger, J. *Chem. Soc. Rev.* **1999**, *28*, 279–291. (d) Heath, J. R., Ed. *Acc. Chem. Res.* **1999**, *32*, 388 (Special issue on Nanoscale Materials). (e) Zaworotko, M. J. *Nature* **1999**, *402*, 242–243. (f) *Perspectives in Supramolecular Chemistry*; *Supramolecular Materials and Technologies*; Reinhoudt, D. N., Ed.; Wiley: Chichester, 1999; Vol. 4.

2. Scaiano, J. C.; Garcia, H. *Acc. Chem. Res.* **1999**, *32*, 783–793.

3. Kumar, V. S. S.; Kuduva, S. S.; Desiraju, G. R. J. *Chem. Soc., Perkin Trans. 2* **1999**, 1069–1073.

4. (a) Bishop, R. *Chem. Soc. Rev.* **1996**, 311–319. (b) Aoyama, Y. *Top. Curr. Chem.* **1998**, *98*, 131–161. (c) Yaghi, O. M.; Li, H.; Davis, C.; Richardson, D.; Groy, T. L. *Acc. Chem. Res.* **1998**, *31*, 474–484. (d) MacGillivray, L. R.; Atwood, J. L. *Angew. Chem., Int. Ed.* **1999**, *38*, 1018–1033.

5. Desiraju, G. R. *Angew. Chem., Int. Ed. Engl.* **1995**, *34*, 2311–2327.

6. Fyfe, M. C. T.; Stoddart, J. F. *Acc. Chem. Res.* **1997**, *30*, 393–401.

7. (a) Brunet, P.; Simard, M.; Wuest, J. D. *J. Am. Chem. Soc.* **1997**, *119*, 2737–2738. (b) MacGillivray, L. R.; Atwood, J. L. *J. Am. Chem. Soc.* **1997**, *119*, 6931–6932. (c) Jetti, R. K. R.; Kuduva, S. S.; Reddy, D. S.; Xue, F.; Mak, T. C. W.; Nangia, A.; Desiraju, G. R. *Tetrahedron Lett.* **1998**, *39*, 913–916. (d) Swift, J. A.; Pivovar, A. M.; Reynolds, A. M.; Ward, M. D. *J. Am. Chem. Soc.* **1998**, *120*, 5887–5894. (e) Aakeröy, C. B.; Beatty, A. M.; Leinen, D. S. *Angew. Chem., Int. Ed.* **1999**, *38*, 1815–1819. (f) Ranganathan, A.; Pedireddi, V. R.; Rao, C. N. R. *J. Mater. Chem.* **1999**, *9*, 2407–2411. (g) Heo, J.; Kim, S.-Y.; Whang, D.; Kim, K. *Angew. Chem., Int. Ed.* **1999**, *38*, 641–643; (h) Chui, S. S.-Y.; Lo, S. M.-F.; Charmant, J. P. H.; Orpen, A. G.; Williams, I. D. *Science* **1999**, *283*, 1148–1150. (i) Jetti, R. K. R.; Xue, F.; Mak, T. C. W.; Nangia, A. *J. Chem. Soc., Perkin Trans. 2* **2000**, 1223–1232.

8. (a) Palmans, A. R. A.; Vekemans, J. A. J. M; Kooijman, H.; Spek, A. L.; Meijer, E. W. *Chem. Commun.* **1997**, 2247–2248. (b) Imakubo, T.; Maruyama, T.; Sawa, H.; Kobayashi, K. *Chem. Commun.* **1998**, 2021–2022. (c) Allock, H. R.; Primrose, A. P.; Sunderland, N. J.; Rheingold, A. L.; Guzei, I. A.; Parvez, M. *Chem. Mater.* **1999**, *11*, 1243–1252. (d) Kiang, Y.-H.; Gardner, G. B.; Lee, S.; Xu, Z.; Lobkovsky, E. B. *J. Am. Chem. Soc.* **1999**, *121*, 8204–8215.

9. (a) Hulliger, J. *Z. Kristallogr.* **1998**, *213*, 441–444. (b) Hulliger, J. *Z. Kristallogr.* **1999**, *214*, 9–13.

10. Hu, J.; Odom, T. W.; Lieber, C. M. *Acc. Chem. Res.* **1999**, *32*, 435–445. (b) Yao, Z.; Postma, H. W. Ch.; Balents, L.; Dekker, C. *Nature* **1999**, *402*, 273–276.

11. Jetti, R. K. R.; Xue, F.; Mak, T. C. W.; Nangia, A. *Cryst. Eng.* **1999**, *2*, 215–224.

12. (a) Pedireddi, V. R.; Reddy, D. S.; Goud, B. S.; Craig, D. C.; Rae, A. D.; Desiraju, G. R. *J. Chem. Soc., Perkin Trans. 2* **1994**, 2353–2360. (b) Robinson, J. M. A.; Kariuki, B. M.; Harris, K. D. M.; Philp, D. *J. Chem. Soc., Perkin Trans. 2* **1998**, 2459–2469.

13. Desiraju, G. R.; Steiner, T. *The Weak Hydrogen Bond in Structural Chemistry and Biology*; Oxford University Press: Oxford, 1999.

14. Desiraju, G. R.; Sarma, J. A. R. P. *Proc. Ind. Acad. Sci. (Chem. Sci.)* **1986**, *96*, 599–605.

15. Lommerse, J. P. M.; Stone, A. J.; Taylor, R.; Allen, F. H. *J. Am. Chem. Soc.* **1996**, *118*, 3108–3116.

16. Allen, F. H. *Acta Crystallogr. Sect. A* **1998**, *54*, 758–771.

17. (a) Gavezzotti, A. *Chem. Phys. Lett.* **1989**, *161*, 67–72. (b) Zhang, J.; Moore, J. S. *J. Am. Chem. Soc.* **1992**, *114*,

9701–9702. (c) Cozzi, F.; Cinquini, M.; Annunziata, R.; Dwyer, T.; Siegel, J. S. *J. Am. Chem. Soc.* **1992**, *114*, 5729–5733.
18. Thalladi, V. R.; Panneerselvam, K.; Carrell, C. J.; Carrell, H. L.; Desiraju, G. R. *J. Chem. Soc., Chem. Commun.* **1995**, 341–342.
19. Dunitz, J. D. *The Crystal as a Supramolecular Entity*. In *Perspectives in Supramolecular Chemistry*; Desiraju, G. R., Ed.; Wiley: Chichester, 1995; Vol. 2; pp. 1–30.
20. Another example of a similar phenomenon is found in the perhydrotriphenylene host–guest structures. Its chloroform solvate ($P6_3/m$) has unit-cell dimensions $a=b=25.08$ Å, $c=4.78$ Å while in the cyclohexane clathrate ($R\bar{3}$) *a*- and *b*-axes are nearly the same (25.55 Å) but the *c*-axis is 9 times longer (43.02 Å). In the cyclohexane adduct, the super unit cell contains 54 host and 21 guest molecules. See Ref. 1a, pp. 375–377.
21. (a) Kobayashi, K.; Shirasaka, T.; Yamaguchi, K.; Sakamato, S.; Horn, E.; Furukawa, N. *Chem. Commun.* **2000**, 41–42. (b) Chopra, N.; Naumann, C.; Sherman, J. C. *Angew. Chem., Int. Ed.* **2000**, *39*, 194–196.
22. Forkey, D. M.; Attar, S.; Noll, B. C.; Koerner, R.; Olmstead, M. M.; Balch, A. L. *J. Am. Chem. Soc.* **1997**, *119*, 5766–5767.
23. Hayashi, N.; Kuruma, K.; Mazaki, Y.; Imakubo, T.; Kobayashi, K. *J. Am. Chem. Soc.* **1998**, *120*, 3799–3800.
24. Nangia, A.; Desiraju, G. R. *Chem. Commun.* **1999**, *605*, 606.
25. Nangia, A.; Desiraju, G. R. *Acta Crystallogr. Sect. A* **1998**, *54*, 934–944.
26. Schafer, F. C.; Thurston, J. T.; Dudley, J. R. *J. Am. Chem. Soc.* **1951**, *73*, 2990–2992.
27. (a) Higashu, T. *ABSCOR: An Empirical Absorption Correction Based on Fourier Coefficient Fitting*; Rigaku Corporation: Tokyo, 1995. (b) Sheldrick, G. M. *SADABS: Program for Empirical Absorption Correction of Area Detector Data*; University of Göttingen, Germany, 1996. (c) Kopfmann, G.; Huber, R. *ψ-scan: Acta Crystallogr. A* **1968**, *24*, 348–351.
28. (a) Sheldrick, G. M. *SHELXS-97: Program for the Solution of Crystal Structures*; University of Göttingen, Germany, 1997. (b) Sheldrick, G. M. *SHELXL-97: Program for the Refinement of Crystal Structures*; University of Göttingen, Germany, 1997.